The disease-protective complement factor H allotypic variant Ile62 shows increased binding affinity for C3b and enhanced cofactor activity.

Agustín Tortajada[1], Tamara Montes[1], Ruben Martinez-Barricarte[1], B. Paul Morgan[2], Claire L. Harris[2,*] and Santiago Rodríguez de Córdoba[1,*].

1) Centro de Investigaciones Biológicas, Consejo Superior de Investigaciones Científicas, Centro de Investigación Biomédica en Enfermedades Raras and Instituto Reina Sofía de Investigaciones Nefrológicas, Ramiro de Maeztu 9, 28040 Madrid, Spain.

2) Department of Medical Biochemistry and Immunology, School of Medicine, Cardiff University, Cardiff, CF14 4XN, UK.

**)* These two authors contributed equally to this work.

Corresponding authors:

Dr. Santiago Rodríguez de Córdoba,
Complement Genetics and Molecular Pathology Unit,
Depart. of Cellular and Molecular Physiopathology,
Centro de Investigaciones Biologicas,
Ramiro de Maeztu 9,
Madrid 28040, Spain.
Tel: (+34) 91 7373112 x4432
Fax: (+34) 91 5360432
E-mail: srdecordoba@cib.csic.es

Dr. Claire L Harris,
Complement Biology Group,
Depart. of Medical Biochemistry and Immunology,
School of Medicine,
Cardiff University,
Henry Wellcome Building,
Heath Park, Cardiff, CF14 4XN, UK.
Tel: (+44) 29 20687012
Fax: (+44) 29 20687079
E-mail: HarrisCL@cardiff.ac.uk

Summary

Mutations and polymorphisms in the gene encoding factor H (*CFH*) have been associated with atypical haemolytic uraemic syndrome, dense deposit disease and age-related macular degeneration. The disease-predisposing *CFH* variants show a differential association with pathology that has been very useful to unravel critical events in the pathogenesis of one or other disease. In contrast, the fH-Ile_{62} polymorphism confers strong protection to all three diseases. Using ELISA-based methods and surface plasmon resonance analyses we show here that the protective fH-Ile_{62} variant binds more efficiently to C3b than fH-Val_{62} and competes better with factor B in proconvertase formation. Functional analyses demonstrate an increased cofactor activity for fH-Ile_{62} in the factor I-mediated cleavage of fluid phase and surface-bound C3b; however, the two fH variants show no differences in decay accelerating activity. From these data we conclude that the protective effect of the fH-Ile_{62} variant is due to its better capacity to bind C3b, inhibit proconvertase formation and catalyse inactivation of fluid-phase and surface-bound C3b. This demonstration of the functional consequences of the fH-Ile_{62} polymorphism provides relevant insights into the complement regulatory activities of fH that will be useful in disease prediction and future development of effective therapeutics for disorders caused by complement dysregulation.

Introduction

Complement is a major component of innate immunity with crucial roles in microbial killing, apoptotic cell clearance and immune complex handling. Activation of complement by foreign surfaces (alternative pathway; AP), antibody (classical pathway; CP) or mannan (lectin pathway; LP), causes target opsonisation, leukocyte recruitment, and cell lysis. The critical steps in complement activation are the formation of unstable protease complexes, named C3-convertases (AP, C3bBb; CP/LP, C4b2a) and the cleavage of C3 to generate C3b. Convertase-generated C3b can form more AP C3-convertase, providing exponential amplification to the initial activation. Binding of C3b to the C3-convertases generates the C5-convertases with the capacity to bind and cleave C5, initiating formation of the lytic membrane attack complex (MAC).

Nascent C3b binds indiscriminately to pathogens and adjacent host cells. To prevent damage to self and to avoid wasteful consumption of components, complement is under the control of multiple regulatory proteins that limit complement activation by inactivating C3b or C4b, dissociating the multimolecular C3/C5 convertases or inhibiting MAC formation. In health, activation of C3 in the blood is kept at a low level and deposition of C3b and further activation of complement is limited to the surface of pathogens (1).

Factor H (fH) is a relatively abundant plasma protein that is essential to maintain complement homeostasis and to restrict the action of complement to activating surfaces. fH binds to C3b, accelerates the decay of the alternative pathway C3-convertase (C3bBb) and acts as a cofactor for the fI-mediated proteolytic inactivation of C3b (2-4). fH regulates complement both in fluid phase and on cellular surfaces (5-7). The factor H molecule is a single polypeptide chain glycoprotein of 155 kDa composed of 20 repetitive units of ~60

amino acids (8), named short consensus repeats (SCR), arranged end-to-end like 'beads on a string'. fH presents different interaction sites for C3b and polyanions which delineate distinct functional domains at the N- and C-termini. The C3b binding site in SCR1-4 is the only site essential for the C3-convertase decay accelerating and fI cofactor activities of fH. Similarly, the C3b/polyanion-binding site located within SCR19-20 is the most important site for preventing alternative pathway activation through binding to host cell membranes (9).

Several reports in the last few years have established that membranoproliferative glomerulonephritis type II or dense deposit disease (MPGN2/DDD) (10-13), atypical haemolytic uraemic syndrome (aHUS) (14-17) and age-related macular degeneration (AMD) (18-21), are each associated with mutations or polymorphisms in the *CFH* gene. The available data support the hypothesis that AP dysregulation is a unifying pathogenetic feature of these diverse conditions. They also illustrate a remarkable genotype-phenotype correlation in which distinct genetic variations at *CFH* specifically predispose to aHUS, AMD or MPGN2. In addition to these *CFH* variants conferring increased risk to disease, one common extended haplotype in the *CFH* gene has been described associated with lower risk to aHUS, AMD and MPGN2/DDD (18, 22). This *CFH* haplotype carries the Ile_{62} variant within the SCR1 domain in the N-terminal region that is essential for fH regulatory activities. It is, therefore, possible that the substitution of Val for Ile at position 62 may increase the fH regulatory activity and thus confer lower risk to AMD, MPGN2/DDD and aHUS by reducing AP activation.

To test this hypothesis we have purified the two fH variants from the plasma of fH-Val_{62} and fH-Ile_{62} homozygote donors and performed a series of binding and functional analyses. Our data show that the fH-Ile_{62} variant exhibits increased binding to C3b

compared to fH-Val62, and is also a more efficient cofactor for fI in the proteolytic inactivation of C3b. Together these data provide an explanation for why fH-Ile62 protects from diseases associated with AP dysregulation.

Results

Interaction of fH-Ile$_{62}$ and fH-Val$_{62}$ with surface-bound C3b

Purified C3b was immobilized on microtiter plates and serial dilutions of fH-Ile$_{62}$ or fH-Val$_{62}$ variants, 'polished' free from potential aggregates by gel filtration, were allowed to interact with C3b for two hours at 37ºC. Factor H bound to C3b was detected using an antifH mAb (35H9) that recognises equally both variants as described in Materials and Methods. Binding of the protective fH-Ile$_{62}$ variant to surface-bound C3b was significantly higher than that of the fH-Val$_{62}$ variant ($P<0.0001$) (Figure 1a). These data suggest that the Val62Ile polymorphism influences the interaction between fH and C3b. To confirm these findings in a different assay, we performed SPR studies using chips coated with identical amounts of fH-Ile$_{62}$ or fH-Val$_{62}$ variants and flowed increasing concentrations of C3b. These SPR assays replicated and extended the findings from ELISA experiments, showing that fH-Ile$_{62}$ binds C3b with a higher affinity than fH-Val$_{62}$ (Figure 2a). Steady state analysis under defined buffer conditions gave a K_D of 1.04μM for fH-Ile$_{62}$ and 1.33μM for fH-Val$_{62}$ (Figure 2b).

Cofactor activity for fI-mediated proteolysis of fluid phase C3b

In order to study the fI cofactor activity of the fH-Ile$_{62}$ and fH-Val$_{62}$ variants we first performed a fluid phase cofactor activity assay. Identical amounts of purified fH-Ile$_{62}$ and fH-Val$_{62}$ variants were added to purified C3b in the presence of fI and incubated for 2.5, 5, 7.5 and 10 minutes at 37ºC. Under the conditions of these experiments 100% of C3b cleavage was reached after 20 minutes of incubation. Controls for 0% cleavage were obtained in the absence of fI. The ratio between α´chain / βchain of C3b, determined by

densitometry, was used to determine the percentage of C3b cleavage. Figure 3a illustrates one experiment representative of several, showing that the fH-Ile_{62} variant is more efficient as a cofactor for fI in the cleavage of C3b in the fluid phase. Figure 3b shows a significant difference (P=0.0012) in the % C3b cleavage catalysed by identical amounts of purified fH-Ile_{62} and fH-Val_{62} variants at different incubation times. Double regression plotting and statistical analysis of the slopes for the linearized curves reveal significant differences between the cofactor activities of the fH-Ile_{62} and fH-Val_{62} variants. Figure 3c shows the densitometry analysis for the differences in cofactor activities between the fH-Ile_{62} and fH-Val_{62} variants at 6 minutes incubation time in an independent set of assays. From these experiments it was calculated that fH-Ile_{62} is approximately 20% more active than fH-Val_{62} as a cofactor for the fI-mediated cleavage of fluid phase C3b.

Cofactor activity of fI-mediated inactivation of surface-bound C3b.

To determine whether the fH-Ile_{62} variant is also more active than fH-Val_{62} as cofactor for the fI-mediated inactivation of surface-bound C3b we used a haemolytic assay. C3b deposited onto sheep erythrocytes was subjected to degradation by fI in the presence of increasing amounts of purified fH-Ile_{62} or fH-Val_{62}. For each fH concentration, the residual surface-bound C3b was determined by measuring sheep erythrocyte lysis after lytic pathway reconstitution (see Materials and Methods).

Three different experiments, each in triplicate, were performed with identical results (Figure 4). Calculated EC50 were 22.6nM and 14nM for fH-Ile_{62} and fH-Val_{62}, respectively. These experiments consistently show that fH-Ile_{62} is significantly more active than fH-Val_{62} as a cofactor for the fI-mediated proteolysis of surface bound C3b (P=0.0025; two-tailed unpaired T test). From these experiments it was estimated that the

dose of fH-Val_{62} needed to achieve 50% fI-mediated inactivation of C3b is 1.6-1.8 fold that required when fH-Ile_{62} is used.

Decay accelerating activity of the alternative pathway C3-convertase.

To measure AP convertase decay accelerating activity of the fH-Ile_{62} and fH-Val_{62} variants, sheep erythrocytes were coated with AP convertase (C3bBb) and incubated with increasing amounts of purified fH-Ile_{62} or fH-Val_{62} in the absence of fI. Residual AP convertase on the sheep erythrocytes was determined by measuring erythrocyte lysis after lytic pathway reconstitution (see Materials and Methods). In three independent experiments, these hemolytic assays showed that fH-Ile_{62} and fH-Val_{62} have equivalent decay accelerating activity (Figure 5a). Independent confirmation of this finding was sought using Biacore (Figure 5b). AP C3 convertase was assembled on a C3b-coated chip and allowed to decay naturally for 160 seconds; fH-Ile_{62} or fH-Val_{62} at a concentration of 73nM were then flowed over the chip. Binding of fH and accelerated convertase decay occurred simultaneously. Following dissociation of fH from the surface, remaining convertase was measured, this was identical for each fH variant. Note the increased binding of fH-Ile_{62} to the surface in agreement with Figure 2a.

Competition between fH and fB for binding to C3b

From the experiments presented above it is clear that the differences in binding affinity for C3b of the fH-Ile_{62} and fH-Val_{62} variants affect their capacity to function as cofactor for fI in the proteolysis of C3b. To explore whether these differences in affinity also influence the ability of fH to prevent formation of the C3 proconvertase by competing with fB for binding to C3b competition assays were performed on Biacore. We first

showed, in keeping with previous reports, that fH does not accelerate decay of the pre-formed proconvertase C3bB (Figure 6a). When fB together with increasing amounts of fH was flowed over a C3b surface, competition between fB and fH for binding to C3b was apparent from the fH-dependent decrease in the formation of proconvertase measured following dissociation of fH (Figure 6b). Next, fB was flowed over C3b and binding competed using identical amounts of the fH-Ile_{62} and fH-Val_{62} variants. As expected, fH-Ile_{62}, shown to bind better to C3b, was a more efficient competitor and caused a small but consistent decreased formation of the proconvertase (Figure 6c). These data illustrate that the increased C3b-binding affinity of the fH-Ile_{62} variant makes it not only a better cofactor for the fI-dependent inactivation of C3b, but also a more efficient inhibitor of the formation of the C3 proconvertase.

Combined effects of the fH Val62Ile and fB Arg32Gln polymorphisms in the formation of the AP C3 convertase.

Previously, we have characterized the common fB polymorphism, fB-Arg_{32}/fB-Gln_{32}/fB-Trp_{32}, and found that the AMD-protective allele fB-Gln_{32} had decreased affinity for C3b compared with the fB-Arg_{32} and fBTrp_{32} alleles. SPR comparison revealed markedly different proenzyme formation activities; fB-Arg_{32} bound C3b with 4-fold higher affinity than fB-Gln_{32}, and formation of activated convertase was enhanced (29). Here we tested combinations of these two variants of fB with the two variants of fH characterised above in order to explore the consequences of different combinations of variant components and regulators. In haemolytic assays, we found that the combinations complemented each other as predicted from their individual activities (Figure 7). The fH-Ile_{62}-fB-Gln_{32} combination was the least lytic and the fH-Val_{62}-fB-Arg_{32} combination the

most lytic (Figure 7). Calculated EC50s were 4.3nM and 3.5nM (for the fH-Ile_{62}-fB-Gln_{32} and fH-Val_{62}-fB-Gln_{32} combinations, respectively) and 3nM and 2.1nM (for the fH-Ile_{62}-fB-Arg_{32} and fH-Val_{62}-fB-Arg_{32} combinations, respectively). Differences in the EC50 were statistically significant between the combinations fH-Val_{62}-fB-Arg_{32} and fH-Ile_{62}-fB-Gln_{32} ($P<0.001$); fH-Val_{62}-fB-Arg_{32} and fH-Ile_{62}-fB-Arg_{32} ($P=0.004$); and fH-Val_{62}-fB-Gln_{32} and fH-Ile_{62}-fB-Gln_{32} ($P=0.034$). P values were calculated using a two-tailed unpaired T test. No significant differences were observed between the combinations fH-Val_{62}-fB-Gln_{32} and fH-Ile_{62}-fB-Arg_{32}.

Discussion

Factor H (fH) plays a key role in regulating the alternative pathway by acting as a cofactor for fI-mediated cleavage of C3b to iC3b, by accelerating the dissociation of the alternative pathway C3 convertases and by competing with factor B for binding to C3b in proconvertase formation (9). All these activities are mediated by the interaction between fH and C3b. Functional studies using truncated molecules have demonstrated that fH possesses binding sites for C3b located at the N-terminus (SCR1-4), the C-terminus (SCR19-20) and in the middle of the molecule (SCR7) (30, 31). The C3b-binding sites at the C-terminal and N-terminal ends are well characterized, whereas that in SCR7 is a very weak binding site of unknown function. The C3b-binding site in SCR19-20 shows the highest affinity for C3b and plays a critical role in recognition of foreign surfaces by fH. At the other end of the molecule, the C3b-binding site in SCR1-4 is essential for the regulatory activities of fH as it carries the fI-mediated cofactor and decay-accelerating activities of fH. Deletion mutagenesis studies have demonstrated that the N-terminal four SCRs are necessary and sufficient for these activities of fH, suggesting that multiple interactions occur between C3b and the N-terminal region of fH (32, 33).

Here we report that the Val62Ile substitution in SCR1 of fH increases its affinity for C3b; as a consequence, when compared to fH-Val_{62}, fH-Ile_{62} competes more efficiently with fB for C3b binding in proconvertase formation and acquires enhanced cofactor activity for the factor-I mediated cleavage of C3b proteolysis; however, its decay accelerating activity is not altered. These findings show that fH-Ile_{62} is a better AP convertase inhibitor and provide an explanation for the association of the fH-Ile_{62} variant with protection in three distinct disorders linked by AP dysregulation. The fact that the Val62Ile substitution

affects binding to C3b but not decay accelerating activity suggests that different regions in fH may be involved in binding C3b/cofactor activity and in decay accelerating activity.

SCR1 is necessary for both cofactor and decay accelerating activities (32, 33). Our findings imply that the C3b-binding site in SCR1 is not directly involved in decay accelerating activity and that SCR1 may contain distinct, although perhaps overlapping, sites for cofactor and decay accelerating activities. This scenario dictates that the interactions of fH with C3b and with C3bBb are structurally distinct. Previously, we showed that the aHUS-associated fB mutation, K323E, located remote from the C3b-fB interaction site, makes the C3bBb convertase resistant to decay by decay accelerating factor (DAF) and fH (24, 34). The mutation apparently affects a complement regulator binding site in the von Willebrand factor type A (vWA) domain of fB (24). We have also previously showed that DAF-SCR2 interacts with Bb, whereas DAF-SCR4 interacts with C3b in the C3bBb complex (27). From comparison with DAF it is likely that decay accelerating activity of fH also requires binding to both Bb and C3b. We suggest that there are two distinct binding sites in SCR1, one including the Val62Ile fH polymorphism that is necessary for cofactor activity, and a second that binds fB at, or close to, K323 in fB that is essential for decay accelerating activity. We also postulate that fH has a C3b binding site in SCR3/SCR4 that contributes to both cofactor and decay accelerating activities.

Overwhelming evidence has associated MPGN2/DDD, aHUS and AMD with mutations or polymorphisms in the *CFH* gene and provided conclusive data that AP dysregulation is a unifying pathogenetic feature of these diverse conditions (35). However, only MPGN2/DDD and AMD have pathological similarities. Indeed, occasionally, they occur in the same patient (36). The hallmark of AMD is drusen, a complex, complement-containing material that accumulates beneath the retinal pigmented epithelium; in

MPGN2/DDD, accumulation of a drusen-like C3 and electron-dense material occurs along the glomerular basement membrane (GBM). In contrast to these 'debris-associated' conditions, aHUS is characterized by renal endothelial cell injury and thrombosis (thrombotic microangiopathy), resulting in haemolytic anaemia, thrombocytopenia and renal failure. Consistent with these differences, distinct functional alterations in fH associate with pathogenesis in these disorders. Mutations or polymorphisms altering the C3b/polyanions-binding site located at the C–terminal region of fH are strongly associated with aHUS because they impair the capacity of fH to protect host cells but have no effect on fluid-phase fH activities. On the other hand, mutations that disrupt the capacity of fH to inhibit complement activation in plasma result in massive activation of C3 that causes MPGN2/DDD. This clear genotype-phenotype correlation contrasts with the association of the fH Val62Ile polymorphism, associated with lower risk for the three diseases (18, 22).

To understand why the fH-Ile_{62} variant confers protection from aHUS, MPGN2/DDD and AMD, we purified to homogeneity both fH-Val_{62} and fH-Ile_{62} variants and compared in a series of functional assays for potential effects on proenzyme formation and cofactor and decay accelerating activities in fluid phase and on cell surfaces. Using four different experimental approaches, we showed that fH-Ile_{62} binds better to C3b, competes better with fB to reduce proenzyme formation, and performs more efficiently as a cofactor of fI in the proteolysis of fluid phase and surface-bound C3b. These enhanced activities explain the protective role of fH-Ile_{62} both in diseases associated with fluid phase complement dysregulation, like MPGN2/DDD, and membrane-restricted dysregulation as is the case in aHUS.

One important conclusion from this report is that the protective effect of the fH-Ile_{62} variant is subtle, with alterations in activities of between 20% and 50% depending on the

assay used. This is consistent with the recent observation (37) that the Val62Ile polymorphism causes a very minor perturbation in the structure of SCR1, this contrasts with the larger structural disturbance caused by an aHUS-associated mutation (Arg53His) which has detrimental consequences on the functional activities of fH. Nevertheless, the very nature of the complement system will amplify these small effects. Further, as we show here by combining known functional variants in fB with fH-Ile_{62} and fH-Val_{62}, particular combinations of variants in components and regulators will result in very different AP characteristics, markedly affecting formation and regulation of the AP C3 convertase in plasma and on cell surfaces. Identification of individuals carrying 'high risk' or 'low risk' combinations ('complotypes') of the polymorphic complement component and regulator variants will be of great importance for prediction of disease risk and may also help in diagnosis and choice of treatment for diseases involving complement dysregulation.

Materials and Methods

Purification of complement components and activation fragments

Normal healthy volunteers were screened for mutations/polymorphisms in the *CFH* gene by automatic DNA sequencing of PCR amplified fragments. Genomic DNA was prepared from peripheral blood cells according to standard procedures (23). Each exon of the *CFH* gene was amplified from genomic DNA by using specific primers derived from the 5' and 3' intronic sequences as described (14). Automatic sequencing was performed in an ABI 3730 sequencer using a dye terminator cycle sequencing kit (Applied Biosystems, Foster City, CA).

Factor H was purified from individuals homozygous for either the fH-Ile_{62} and fH-Val_{62} variants who were identical at all other amino acid residues. Fresh EDTA plasma (100 ml) was precipitated with 7% polyethylene glycol 8000 overnight at 4ºC. The precipitate was re-dissolved in PBS, dialysed extensively against 20 mM Tris-HCl (pH 7.4), 50 mM NaCl, 5 mM EDTA and applied to a heparin-Sepharose column (Heparin 6B Fast Flow, Amersham) equilibrated in the same buffer. The proteins bound to the column were eluted with a 100-200 mM NaCl gradient in 20mM Tris-HCl, pH 7.4, 5mM EDTA. Fractions containing fH were identified by sodium dodecyl sulfate polyacrylamide gel electrophoresis (SDS-PAGE), pooled, dialysed against 20 mM Tris-HCl; pH 7.6, 20 mM NaCl and 10 mM EDTA and applied to a DEAE-Sephacel column. Bound proteins were eluted with a 20-300 mM NaCl gradient. Fractions containing fH were identified by SDS-PAGE, pooled and further purified by gel filtration on a Superose^{TM} 6 10/300 column (GE Healthcare). The fH peak fractions were pooled and stored frozen at -70ºC. The fH used in haemolysis assays and Biacore studies was purified by affinity chromatography using immobilised anti-fH (35H9; in house). Protein was eluted with 0.1M Glycine/HCl pH 2,5

and gel filtered into assay buffer using a Superdex 200 10/300 column (GE Healthcare) immediately prior to analysis. The purity of the final preparations was confirmed by SDS-PAGE. Preparations of fH-Ile_{62} and fH-Val_{62} were obtained without any detectable contaminants or aggregates (Figure 1b).

C3 and Factor B were purified by affinity chromatography and gel filtration as described previously (24). Concentration of proteins was assessed using absorbance at A280, molarities were calculated using an extinction coefficient for fH of 1.95 (25), for fB of 1.43 and for C3 of 0.98 (coefficients were obtained by using Protean Software, DNAStar). C3b was generated by limited digestion with trypsin or convertase as previously described (24, 26) and re-purified by ion exchange and/or gel filtration as described above (GE Healthcare). C3b was obtained without any detectable contaminants or aggregates. Factor I, factor D and properdin were purchased from Comptech (Tyler, TX).

ELISA C3b–binding Assay

The binding of fH variants to surface-bound C3b was determined by ELISA. In a 96-well polystyrene microtiter plate, C3b (5 μg/ml) in coupling buffer (0.1 M $NaHCO_3$ pH 9.5) was coated overnight at 4ºC. The plate was blocked with washing buffer (20 mM Tris, 150 mM NaCl and 0.1% Tween 20) with 1% Bovine Serum Albumin for 1 hour at room temperature (RT). After washing, serial dilutions of fH variants (10μg/ml) in blocking buffer containing 150 mM NaCl, 5mM EDTA, were added and incubated with surface-bound C3b for 2 hours at 37ºC. After washing, the plate was incubated with anti-fH monoclonal antibody (mAb) 35H9 (in house) in blocking buffer, for 1 hour at RT, and then with a secondary antibody coupled with horseradish peroxidase (DAKO). Colour reaction

was developed with o-phenylene-diamine (DAKO) and absorbance measured at 492nm. fH preparations used in the ligand assay were quantified in duplicate in the same ELISA plate using immobilised polyclonal anti-fH antibody to capture fH and the same anti-fH mAb, 35H9, and secondary antibodies to measure the amount of protein. Concentrations of fH were calculated from curves obtained using purified standard samples.

Biosensor Analysis

Kinetic analyses (Figure 2) were carried out on a Biacore T100, all other analyses were carried out using a Biacore 3000 (GE Healthcare). To measure affinity, fH was amine coupled to a CM5 (carboxymethylated dextran) chip as instructed by the manufacturer (NHS/EDC coupling kit). Number of RUs loaded for both variants were 1004RU (fH Ile62) and 1003RU (fH Val62). C3b was flowed across the surface at different concentrations and bound protein was allowed to decay naturally, the buffer was 10mM Hepes pH7.4, 100mM NaCl, 0.005% Surfactant P20. Data were collected at 25°C at a flow rate of 30µl/minute and were double-referenced (data from reference cell and blank inject were subtracted) to control for bulk refractive index changes. To calculate Kd values (Figure 2) we repeated this experiment on three different surfaces: twice with C3b flowing, and once with hydrolysed C3 flowing. Pooling the data from different runs is difficult. However, the ratio of the derived Kd values was the same for each run as follows: fH-Ile62 was 0.77, 0.78 or 0.8 fold lower than the fH-Val62 form. We flowed C3b over the surface (rather than fH over C3b) in order to minimise the avidity effects seen when flowing fH over the surface. In order to obtain the best quality data, the C3b was gel-filtered prior to use to remove any aggregates and then used in the experiment without further concentration. The C3b needed

to be at a very high concentration pre-filtration in order to achieve 1mg/ml post-filtration, this was the maximum concentration that we could use without precipitating the protein pre-filtration. Although we did not achieve saturation in these experiments, in each case the concentration of C3b used exceeded the Kd value (2.2-fold for fH-Ile62 and 1.7-fold for fH-Val62).

In the following experiments the buffer was 10mM Hepes pH 7.4, 150mM NaCl, 1mM Mg^{2+}. To test the decay activity of fH (Figure 5), fB at 100μg/ml (1.1μM) and fD (2μg/mL), were flowed across the C3b surface to form the AP C3 convertase as previously described (27). The fH variants were subsequently flowed across the C3b surface at 11.3μg/ml (73nM) and decay was monitored. To examine competition between fH and fB for binding to C3b (Figure 6), both proteins were mixed at the indicated concentrations and flowed at 30μl/min across the C3b surface in the absence of fD. To determine whether fH accelerated decay of the proenzyme, fH was flowed over the surface subsequent to the fB injection rather than being premixed.

Cofactor activity for fI-mediated proteolysis of fluid phase C3b

The fluid-phase cofactor activity of factor H was determined in a C3b proteolysis assay using purified proteins. In brief, C3b, fH and fI were mixed in 10mM Hepes pH 7.5, 150mM NaCl, 0.02% Tween 20 at final concentrations of 50 μg/ml (263nM), 4 μg/ml (25.8nM) and 10 μg/ml (114nM), respectively. Mixtures were incubated at 37ºC in a water bath and 20μl aliquots were collected at 2.5, 5, 7.5 and 10 minutes. The reaction was stopped by the addition of 3μl of SDS sample buffer (2% SDS, 62.5mM Tris, 10% Glycerol, 0.75% Bromophenol Blue). Samples were analyzed in 10% SDS-PAGE under

reducing conditions. Gels were stained with Coomassie brilliant blue R-250 (Bio Rad) and proteolysis of C3b determined by measuring the cleavage of the α'-chain using a GS-800 calibrated densitometer (BioRAD) and the MultiGauge software package (FUJIFILM). The C3b β-chain was used as an internal control to normalize the % of cleavage between samples. Percentage of cleavage was determined by the ratio between α´chain / βchain of C3b and setting as 0% the amount of α'-chain at time 0.

Factor H-dependent haemolysis assays

NHS was sequentially depleted of fB and fH (NHSΔBΔH) by flowing over immobilised anti-Bb (JC1 mAb; in house) and immobilised anti-fH (35H9; in house) affinity columns in complement fixation diluent (CFD; Oxoid), undiluted depleted serum was pooled and used in haemolysis assays as described below. Antibody-coated sheep erythrocytes (EA) were prepared by incubating sheep E (2% v/v) with Amboceptor (1/1000 dilution; Behring Diagnostics) in complement fixation diluent (CFD; Oxoid) for 30 minutes at 37ºC, EA were washed and resuspended at 2% (v/v) in CFD. To deposit C3b on the E surface (E-C3b), equal volumes of EA and NHSΔBΔH (8% v/v) were incubated at 37ºC for 10 minutes, the C5 inhibitor (OmCI; 6μg/ml; (28) was added to block the terminal pathway).

To test fH dependent decay accelerating activity, washed E-C3b cells were resuspended to 2% (v/v) in AP buffer (5 mM sodium barbitone pH 7.4, 150 mM NaCl, 7 mM $MgCl_2$, 10 mM EGTA) and AP convertase was formed on the cell surface by incubating with fB 42μg/ml (0.46μM) and fD (0.4μg/ml) at 37ºC for 15 minutes. 1/25

volume of PBS/0.25M EDTA was added to prevent further enzyme formation and cells (50µl) were mixed and incubated with 50µl of fH (serial dilution from 15.4µg/ml (99nM)) in PBS/10mM EDTA for 12 minutes. Lysis was developed by adding 50µl NHSΔBΔH (4%, v/v) in PBS/EDTA and incubating at 37ºC for 20 minutes. To calculate lysis, cells were pelleted by centrifugation, and hemoglobin release was measured by absorbance at 415 nm. Control incubations included 0%lysis (buffer only) and 100%lysis (0.1% Nonidet-P40). Percentage lysis 100*(A415 test sample-A415 0% control)/(A415 100% control-A415 0% control).

To test fH cofactor activity, washed EA-C3b cells were resuspended to 2% in AP buffer and incubated with an equal volume of different concentrations of fH as indicated and constant fI (2.5µg/mL) for 7 minutes at 22ºC. After three washes in AP buffer, 50µl cells (2%) were mixed with 50µl of 70µg/ml fB (0.75µM; fB_{32R} or fB_{32Q}) and fD (0.4µg/ml) and incubated for 10 minutes at 22ºC to form convertase on residual C3b (EA-C3bBb). Lysis was developed by adding 50µl NHSΔBΔH (4%, v/v) in PBS/EDTA and incubating at 37ºC for 20 minutes. Percentage lysis was calculated as described above.

To assess the effect on lysis by combining different polymorphic variants of fB and fH, the above two assays were combined and modified as follows. EA-C3b cells were incubated with 80ng/ml (0.5nM) fH-Ile_{62} or fH-Val_{62} variant and 2.5µg/ml fI for 7 minutes at 22ºC. Washed cells were incubated as described above with different concentrations of $fBArg_{32}$ or $fBGln_{32}$, fD and properdin (1µg/ml) and lysis was developed using NHSΔBΔH.

Acknowledgements

This work was supported by MRC Project Grant Ref 84908 (to CLH and BPM), Ministerio de Ciencia e Innovación Ref SAF 2005-00913 (to SRdeC) the CIBER de Enfermedades Raras and Fundación Renal Iñigo Alvarez de Toledo (to SRdeC). We thank the blood donors for their invaluable contribution to the project.

Author's contributions

CLH, BPM and SRdeC designed research, analysed the data and wrote the paper. CLH and SRdeC contribute equally to this work. AT, TM and RMB prepared the proteins. AT and CLH performed the binding and functional assays.

Conflicts of interest

Authors declare no conflict of interest

References

1. Law, S. and Reid, K. (1995) *Complement.* 2 ed. IRL Press, Oxford, UK.
2. Pangburn, M.K., Schreiber, R.D. and Müller-Eberhard, H.J. (1977) Human complement C3b inactivator: isolation, characterization, and demonstration of an absolute requirement for the serum protein beta1H for cleavage of C3b and C4b in solution. *J. Exp. Med.,* **146**, 257-70.
3. Weiler, J.M., Daha, M.R., Austen, K.F. and Fearon, D.T. (1976) Control of the amplification convertase of complement by the plasma protein beta1H. *Proc. Natl. Acad. Sci. USA,* **73**, 3268-3272.
4. Whaley, K. and Ruddy, S. (1976) Modulation of the alternative complement pathway by beta1H globulin. *J. Exp. Med.,* **144**, 1147-1163.
5. Fearon, D.T. (1978) Regulation by membrane sialic acid of beta1H-dependent decay-dissociation of amplification C3 convertase of the alternative complement pathway. *Proc. Natl. Acad. Sci. USA,* **75**, 1971-1975.
6. Kazatchkine, M.D., Fearon, D.T. and Austen, K.F. (1979) Human alternative complement pathway: Membrane-associated sialic acid regulates the competition between B and beta1H for cell-bound C3b. *J. Immunol.,* **122**, 75-81.
7. Pangburn, M.K., Schreiber, R.D. and Muller Eberhard, H.J. (1983) C3b deposition during activation of the alternative complement pathway and the effect of deposition on the activating surface. *J. Immunol.,* **131**, 1930-1935.
8. Ripoche, J., Day, A.J., Harris, T.J.R. and Sim, R.B. (1988) The complete amino acid sequence of human complement factor H. *Biochem. J.,* **249**, 593-602.
9. Rodriguez de Cordoba, S., Esparza-Gordillo, J., Goicoechea de Jorge, E., Lopez-Trascasa, M. and Sanchez-Corral, P. (2004) The human complement factor H: functional roles, genetic variations and disease associations. *Mol. Immunol.,* **41**, 355-67.
10. Dragon-Durey, M.-A., Fremeaux-Bacchi, V., Loirat, C., Blouin, J., Niaudet, P., Deschenes, G., Coppo, P., Herman Fridman, W. and Weiss, L. (2004) Heterozygous and Homozygous Factor H Deficiencies Associated with Hemolytic Uremic Syndrome or Membranoproliferative Glomerulonephritis: Report and Genetic Analysis of 16 Cases. *J. Am. Soc. Nephrol.,* **15**, 787-795.
11. Levy, M., Halbwachs-Mecarelli, L. and Gubler, M.C. (1986) H deficiency in two brothers with atypical dense intramembranous deposit disease. *Kidney Int.,* **30**, 949-956.
12. Licht, C., Heinen, S., Józsi, M., Löschmann, I., Saunders, R.E., Perkins, S.J., Waldherr, R., Skerka, C., Kirschfink, M., Hoppe, B. *et al.* (2006) Deletion of Lys224 in regulatory domain 4 of Factor H reveals a novel pathomechanism for dense deposit disease (MPGN II). *Kidney Int.,* **70**, 42-50.

13. López-Larrea, C., Dieguez, M.A., Enguix, A., Dominguez, O., Marin, B. and Gómez, E. (1987) A familial deficiency of complement factor H. *Biochem. Soc. T.,* **15**, 648-649.

14. Perez-Caballero, D., Gonzalez-Rubio, C., Esther Gallardo, M., Vera, M., Lopez-Trascasa, M., Rodriguez de Cordoba, S. and Sanchez-Corral, P. (2001) Clustering of missense mutations in the C-terminal region of factor H in atypical hemolytic uremic syndrome. *Am. J. Hum. Genet.,* **68**, 478-484.

15. Caprioli, J., Castelletti, F., Bucchioni, S., Bettinaglio, P., Bresin, E., Pianetti, G., Gamba, S., Brioschi, S., Daina, E., Remuzzi, G. *et al.* (2003) Complement factor H mutations and gene polymorphisms in haemolytic uraemic syndrome: The C-257T, the A2089G and the G2881T polymorphisms are strongly associated with the disease. *Hum. Mol. Genet.,* **12**, 3385-3395.

16. Richards, A., Buddles, M.R., Donne, R.L., Kaplan, B.S., Kirk, E., Venning, M.C., Tielemans, C.L., Goodship, J.A. and Goodship, T.H.J. (2001) Factor H mutations in hemolytic uremic syndrome cluster in exons 18-20, a domain important for host cell recognition. *Am. J. Hum. Genet.,* **68**, 485-490.

17. Warwicker, P., Goodship, T.H.J., Donne, R.L., Pirson, Y., Nicholls, A., Ward, R.M., Turnpenny, P. and Goodship, J.A. (1998) Genetic studies into inherited and sporadic hemolytic uremic syndrome. *Kidney Int.,* **53**, 836-844.

18. Hageman, G.S., Anderson, D.H., Johnson, L.V., Hancox, L.S., Taiber, A.J., Hardisty, L.I., Hageman, J.L., Stockman, H.A., Borchardt, J.D., Gehrs, K.M. *et al.* (2005) A common haplotype in the complement regulatory gene factor H (HF1/CFH) predisposes individuals to age-related macular degeneration. *Proc. Natl. Acad. Sci. USA,* **102**, 7227-7232.

19. Edwards, A.O., Ritter, R., Abel, K.J., Manning, A., Panhuysen, C. and Farrer, L.A. (2005) Complement Factor H Polymorphism and Age-Related Macular Degeneration. *Science,* **308**, 421-424.

20. Haines, J.L., Hauser, M.A., Schmidt, S., Scott, W.K., Olson, L.M., Gallins, P., Spencer, K.L., Kwan, S.Y., Noureddine, M., Gilbert, J.R. *et al.* (2005) Complement Factor H Variant Increases the Risk of Age-Related Macular Degeneration. *Science,* **308**, 419-421.

21. Klein, R.J., Zeiss, C., Chew, E.Y., Tsai, J.-Y., Sackler, R.S., Haynes, C., Henning, A.K., SanGiovanni, J.P., Mane, S.M., Mayne, S.T. *et al.* (2005) Complement Factor H Polymorphism in Age-Related Macular Degeneration. *Science,* **308**, 385-389.

22. Pickering, M.C., Goicoechea de Jorge, E., Martinez-Barricarte, R., Recalde, S., Garcia-Layana, A., Rose, K.L., Moss, J., Walport, M.J., Cook, H.T., Rodriguez de Cordoba, S. *et al.* (2007) Spontaneous hemolytic uremic syndrome triggered by complement factor H lacking surface recognition domains. *J. Exp. Med.,* **204**, 1249-1256.

23. Miller, S.A., Dykes, D.D. and Polesky, H.F. (1988) A simple salting out procedure for extracting DNA from human nucleated cells. *Nucleic Acids Res.,* **16**, 1215.

24. Goicoechea De Jorge, E., Harris, C.L., Esparza-Gordillo, J., Carreras, L., Aller Arranz, E., Abarrategui Garrido, C., Lopez-Trascasa, M., Sanchez-Corral, P., Morgan, B.P. and Rodriguez De Cordoba, S. (2007) Gain-of-function mutations in complement factor B are associated with atypical hemolytic uremic syndrome. *Proc. Natl. Acad. Sci. USA,* **104**, 240-245.

25. Hakobyan, S., Harris, C.L., Tortajada, A., Goicochea de Jorge, E., Garcia-Layana, A., Fernandez-Robredo, P., Rodriguez de Cordoba, S. and Morgan, B.P. (2008) Measurement of factor H variants in plasma using variant-specific monoclonal antibodies: application to assessing risk of age-related macular degeneration. *Invest. Ophthalmol. Vis. Sci.,* **49**, 1983-1990.

26. Sanchez-Corral, P., Anton, L.C., Alcolea, J.M., Marques, G., Sanchez, A. and Vivanco, F. (1989) Separation of active and inactive forms of the third component of human complement C3, by fast protein liquid chromatography (FPLC). *J. Inmunol.,* **122**, 105-113.

27. Harris, C.L., Abbott, R.J.M., Smith, R.A., Morgan, B.P. and Lea, S.M. (2005) Molecular dissection of interactions between components of the alternative pathway of complement and decay accelerating factor (CD55). *J. Biol. Chem.,* **280**, 2569-2578.

28. Hepburn, N.J., Williams, A.S., Nunn, M.A., Chamberlain-Banoub, J.C., Hamer, J., Morgan, B.P. and Harris, C.L. (2007) In Vivo Characterization and Therapeutic Efficacy of a C5-specific Inhibitor from the Soft Tick Ornithodoros moubata. *J. Biol. Chem.,* **282**, 8292-8299.

29. Montes, T., Tortajada, A., Morgan, B.P., Rodriguez de Cordoba, S. and Harris, C.L. (2009) Functional basis of protection against age-related macular degeneration conferred by a common polymorphism in complement factor B. *Proc. Natl. Acad. Sci. USA,* **106**, 4366-4371.

30. Sharma, A.K. and Pangburn, M.K. (1996) Identification of three physically and functionally distinct binding sites for C3b in human complement factor H by deletion mutagenesis. *Proc. Natl. Acad. Sci. USA,* **93**, 10996-11001.

31. Schmidt, C.Q., Herbert, A.P., Kavanagh, D., Gandy, C., Fenton, C.J., Blaum, B.S., Lyon, M., Uhrin, D. and Barlow, P.N. (2008) A new map of glycosaminoglycan and C3b binding sites on factor H. *J. Inmunol.,* **181**, 2610-2619.

32. Kuhn, S., Skerka, C. and Zipfel, P.F. (1995) Mapping of the complement regulatory domains in the human factor H-like protein I and in factor H. *J. Immunol.,* **155**, 5663-5670.

33. Gordon, D.L., Kaufman, R.M., Blackmore, T.K., Kwong, J. and Lublin, D.M. (1995) Identification of complement regulatory domains in human factor H. *J. Immunol.,* **155**, 348-356.

34. Torreira, E., Tortajada, A., Montes, T., Rodriguez de Cordoba, S. and Llorca, O. (2009) 3D structure of the C3bB complex provides insights into the activation and regulation of the complement alternative pathway convertase. *Proc. Natl. Acad. Sci. USA,* **106**, 882-887.

35. Rodriguez de Cordoba, S. and Goicoechea de Jorge, E. (2008) Translational Mini-Review Series on Complement Factor H: Genetics and disease associations of human complement factor H. *Clin. Exp. Immunol.,* **151**, 1-13.

36. Montes, T., Goicoechea de Jorge, E., Ramos, R., Goma, M., Pujol, O., Sanchez-Corral, P. and Rodriguez de Cordoba, S. (2008) Genetic deficiency of complement factor H in a patient with age-related macular degeneration and membranoproliferative glomerulonephritis. *Mol. Immunol.,* **45**, 2897-2904.

37. Hocking, H.G., Herbert, A.P., Kavanagh, D., Soares, D.C., Ferreira, V.P., Pangburn, M.K., Uhrin, D. and Barlow, P.N. (2008) Structure of the N-terminal Region of Complement Factor H and Conformational Implications of Disease-linked Sequence Variations. *J. Biol. Chem.,* **283**, 9475-9487.

Figures

Figure 1. ELISA of fH-Ile$_{62}$ and fH-Val$_{62}$ binding to C3b

(a) Interaction between serial dilutions of purified fH-Ile$_{62}$ (open circles) or fH-Val$_{62}$ (filled circles) with C3b deposited in 96-well plates is expressed as Abs$_{492.}$ Means ± S.D. of three independent experiments are shown. Inset panel shows the double reciprocal plot of the fH-Ile$_{62}$ (open circles) and fH-Val$_{62}$ (filled circles) C3b-binding curves. Multiple linear regression analysis revealed significant differences between Val$_{62}$ and Ile$_{62}$ binding to C3b ($P<0.0001$).

(b) SDS-PAGE illustrating the fH-Ile$_{62}$ and fH-Val$_{62}$ purified from the plasma of homozygote carriers as described in Materials and Methods and then gel filtered to remove aggregates.

Figure 2. SPR analysis of fH-Ile$_{62}$ and fH-Val$_{62}$ binding to C3b.

(a) Identical amounts of fH were immobilised onto a CM5 chip (fH-Ile$_{62}$ 1004RU immobilised; fH-Val$_{62}$ 1003RU immobilised). C3b (2.2μM-8.6nM; 1/2 serial dilution) was flowed across the fH-Ile$_{62}$ or fH-Val$_{62}$ surfaces in 10mm Hepes pH 7.4, 100mM NaCl, 0.005% surfactant P20. Data from a reference cell was subtracted to control for any bulk changes in refractive index. Sensorgrams resulting from fH-Ile$_{62}$ are solid lines and fH-Val$_{62}$ are dotted lines; identical concentrations are illustrated for the two variants.

(b) Steady state analysis of the data in these buffer conditions indicate the affinities for C3b are: K_D fH-Ile$_{62}$: 1.03μM, K_D fH-Val$_{62}$: 1.33μM. The standard errors (SE) in the fits are 0.14μM for fH-Val$_{62}$ and 0.12μM for fH-Ile$_{62}$.

Figure 3. Cofactor activity of fH-Ile$_{62}$ and fH-Val$_{62}$ variants in the proteolysis of fluid phase C3b.

(a) SDS-PAGE of C3b proteolysis. C3b, fH and fI were incubated for the times indicated, the reaction was stopped by the addition of SDS sample buffer. Samples were analyzed by SDS-PAGE under reducing conditions and gels were Coomassie-stained.

(b) Densitometric analysis of C3b proteolysis. Fluid phase cofactor activity was measured be examining C3b cleavage at 2.5, 5, 7.5 and 10 minutes reaction for both fH-Ile$_{62}$ (open circles) and fH-Val$_{62}$ (filled circles) variants. Percentage of cofactor activity was determined by the ratio of cleaved α′chain:βchain, normalized to 0% proteolysis of control samples. Inset panel shows the double reciprocal plot of the fH-Ile$_{62}$ (open circles) and fH-Val$_{62}$ (filled circles) of the cofactor activity curves. Multiple linear regression analysis revealed significant differences between the slopes for fH-Val$_{62}$ and fH-Ile$_{62}$ cofactor activities ($P=0.0012$).

(c) Densitometric analysis of C3b proteolysis from an independent set of assays at 6 minutes incubation time. Difference in percentage of cofactor activity between fH-Val$_{62}$ and fH-Ile$_{62}$ was significant ($P<0.001$).

Figure 4. Cofactor activity of fH-Ile$_{62}$ and fH-Val$_{62}$ variants in the proteolysis of surface-bound C3b.

The ability of the fH variants to mediate fI-catalysed inactivation of surface-bound C3b was assessed using a haemolysis assay. C3b was deposited on the surface of sheep E using the classical pathway as described in Methods. E-C3b were incubated in AP buffer with different concentrations of fH-Ile$_{62}$ (open circles) or fH-Val$_{62}$ (filled circles) and constant fI

for 7 minutes at 22ºC. Cells were washed and AP convertase was formed using purified fB and fD. Lysis was developed in EDTA-containing buffer using serum depleted of fB and fH. Percent lysis was calculated for each concentration of fH. The log10 of fB concentration (final concentration in the incubation) was plotted on the *x* axis, and percentage lysis on the *y* axis. Data points represent mean ±SD of 3 determinations. The curves were fitted by using nonlinear regression analysis to calculate the EC50. There are significant differences (P=0.0025) between the EC50 values corresponding to the fH-Ile_{62} (14nM) and fH-Val_{62} (22.6nM) variants.

Figure 5. Decay accelerating activity of fH-Ile_{62} and fH-Val_{62} variants on surface-bound AP convertase.

The ability of the fH variants to accelerate decay of the AP convertase, C3bBb, was assessed using haemolysis assays with convertase coated sheep E as target (a), and in real time using SPR (b). (a) C3b was deposited on the surface of sheep E using the classical pathway as described in Methods. AP convertase was formed on the cell surface using purified fB and fD, convertase formation was stopped after 15 minutes using EDTA. E-C3bBb were incubated in EDTA with different concentrations of fH-Ile_{62} (open circles) or fH-Val_{62} (filled circles) for 12 minutes to allow decay of the convertase and lysis was developed using serum depleted of fB and fH. Percent lysis was calculated for each concentration of fH. (b) AP convertase was formed on the surface of a C3b-coated Biacore chip by flowing fB and fD over the surface. Convertase decayed naturally for 160s prior to injection of either fH variant (73nM). Change in RU (y-axis) during the fH injection represents the combined effect of fH binding to the surface and to C3bBb, and loss of Bb from the convertase due to fH-mediated accelerated decay. Despite enhanced binding of

fH-Ile$_{62}$ to the surface (grey line), an identical amount of Bb was decayed from the surface as measured following complete dissociation of fH from the chip surface.

Figure 6. Competition between fH and fB for binding to C3b.

(a) Proconvertase was formed on the surface of a C3b-coated Biacore chip by flowing fB, this was allowed to decay naturally for a short time before injection of fH as indicated. As expected, fH did not accelerate decay of the proenzyme. The binding profile of fH on the C3b surface only (no fB injected) is illustrated in grey for comparison. (b) In order to demonstrate competition between fB and fH for binding to the C3b-coated surface, fB (662nM) was flowed across the C3b-coated surface alone (black line), or was premixed with 26 or 66nM fH (dotted grey and solid grey lines respectively) before injection. Note that the change in RU (y-axis) represents the sum of both fB and fH binding to the surface. Decreased proconvertase formation is evident with increasing fH. (c) In order to analyse differential effects of fH-Ile$_{62}$ and fH-Val$_{62}$ on proconvertase formation, 132nM of either variant was premixed with fB (338nM) and injected over the surface. Comparison of binding curves (following dissociation of fH from the surface) with fB binding in the absence of any fH demonstrates that both fH variants prevent proconvertase formation and that the fH-Ile$_{62}$ variant is more effective.

Figure 7. Hemolytic activity of different fH and fB variant combinations.

To test the combined effect of the fH-Ile$_{62}$, fH-Val$_{62}$ and the fBArg$_{32}$, fBGln$_{32}$ variants, C3b was deposited on the surface of sheep E using the classical pathway as described in Methods. E-C3b were incubated in AP buffer with 1nM of fH-Ile$_{62}$ or fH-Val$_{62}$ (final concentration) and constant fI for 7 minutes at 22ºC. Cells were washed and AP convertase

was formed using different concentrations of purified $fBArg_{32}$ or $fBGln_{32}$, and constant fD and properdin. Lysis was developed in EDTA-containing buffer using serum depleted of fB and fH. Percent lysis was calculated for each concentration of fH.

The log10 of fB concentration (final concentration in the incubation) was plotted on the *x* axis, and percentage lysis on the *y* axis. Data points represent mean ±SD of 3 determinations. The curves were fitted by using nonlinear regression analysis to calculate the EC50. Two-tailed unpaired T test showed significant differences in the EC50 between the combinations fH-Val_{62}-fB-Arg_{32} (filled circles) and fH-Ile_{62}-fB-Gln_{32} (open triangles) ($P<0.001$); fH-Val_{62}-fB-Arg_{32} (filled circles) and fH-Ile_{62}-fB-Arg_{32} (open circles) ($P=0.004$); and fH-Val_{62}-fB-Gln_{32} (filled triangles) and fH-Ile_{62}-fB-Gln_{32} (open triangles) ($P=0.034$).

Abbreviations

CFH, gene encoding factor H; AP, alternative pathway; CP, classical pathway; LP, lectin pathway; MAC, membrane attack complex; fH, Factor H; SCR, short consensus repeats; MPGN2/DDD, membranoproliferative glomerulonephritis type II or dense deposit disease; aHUS, atypical haemolytic uraemic syndrome; AMD, age-related macular degeneration; SPR, surface plasmon resonance; fI, factor I; fB, factor B; NHS, normal human serum; CFD, complement fixation diluent; EA, antibody-coated sheep erythrocytes; DAF, decay accelerating factor; vWA, von Willebrand factor type A.

a)

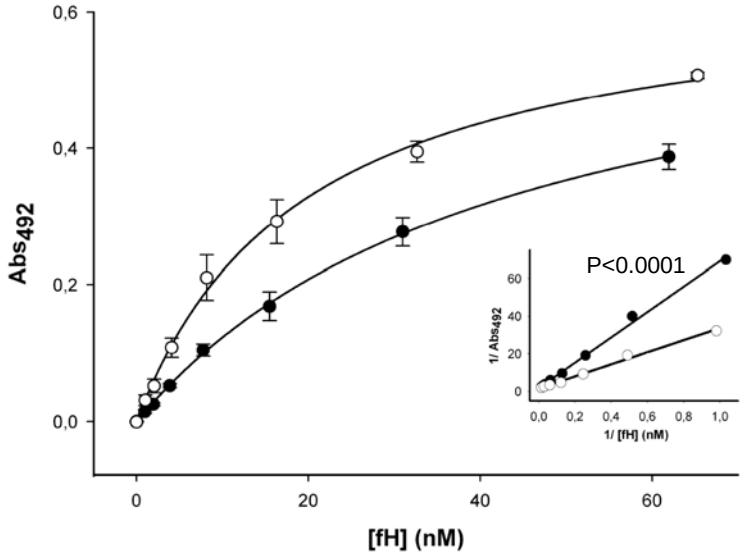
0,6
0,4
0,2
0,0
Abs492
0
20
40
60
[fH] (nM)
P<0.0001
60
40
20
0
1/ Abs492
0,0
0,2
0,4
0,6
0,8
1,0
1/ [fH] (nM)

b)

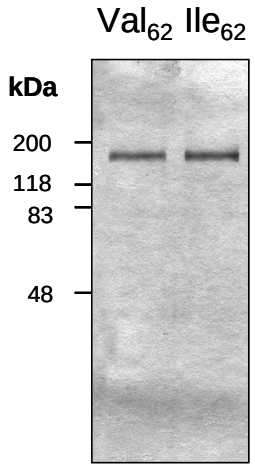
Val62 Ile62
kDa
200
118
83
48

Figure 1

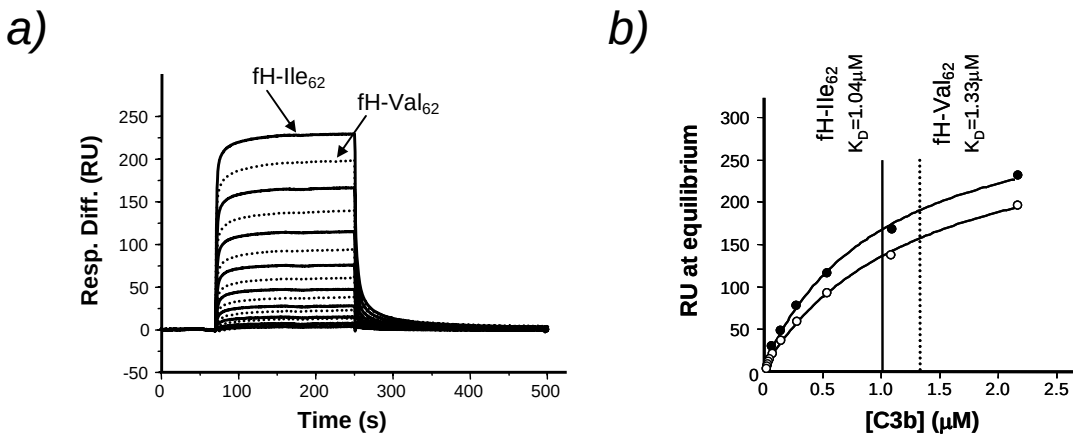
a)
fH-Ile62
fH-Val62
Resp. Diff. (RU)
Time (s)
b)
fH-Ile62
KD=1.04μM
fH-Val62
KD=1.33μM
RU at equilibrium
[C3b] (μM)

Figure 2

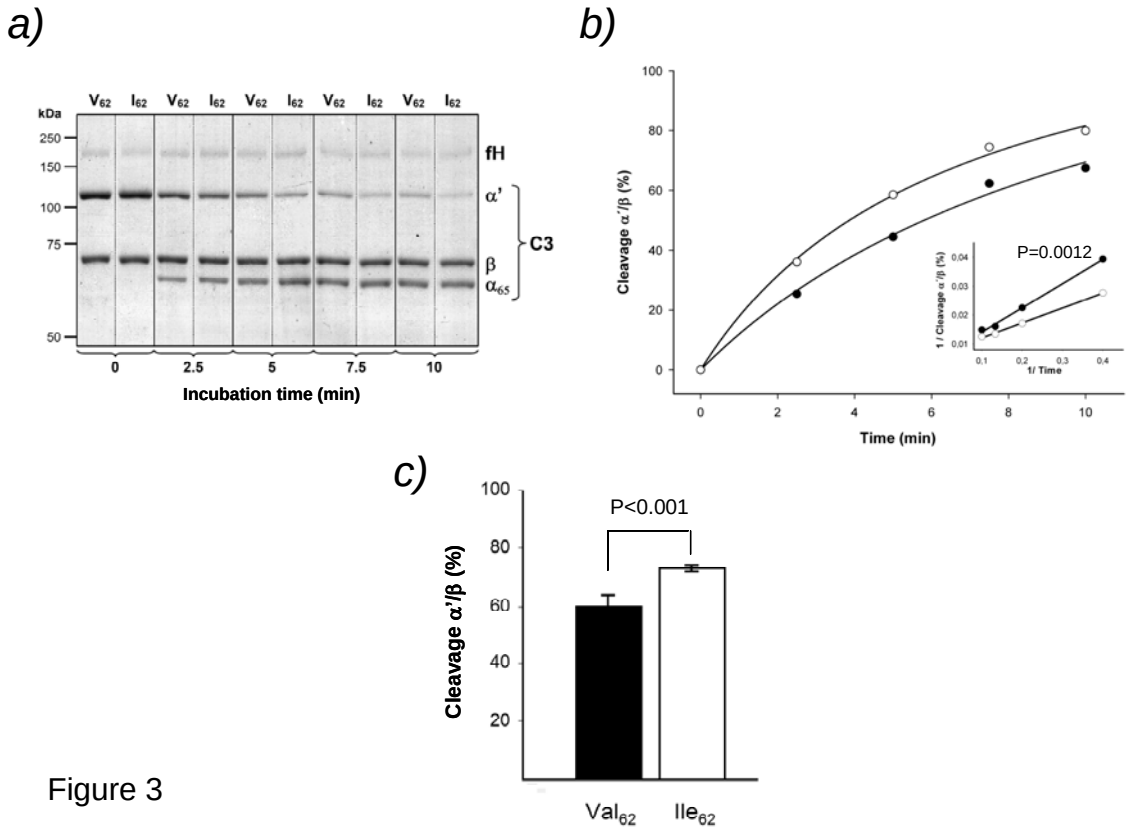
a)
b)
c)
kDa
250
150
100
75
50
V62 I62 V62 I62 V62 I62 V62 I62 V62 I62
fH
α'
β
α65
C3
0
2.5
5
7.5
10
Incubation time (min)
Cleavage α'/β (%)
Time (min)
P=0.0012
1 / Cleavage α'/β (%)
1/ Time
P<0.001
Val62
Ile62

Figure 3

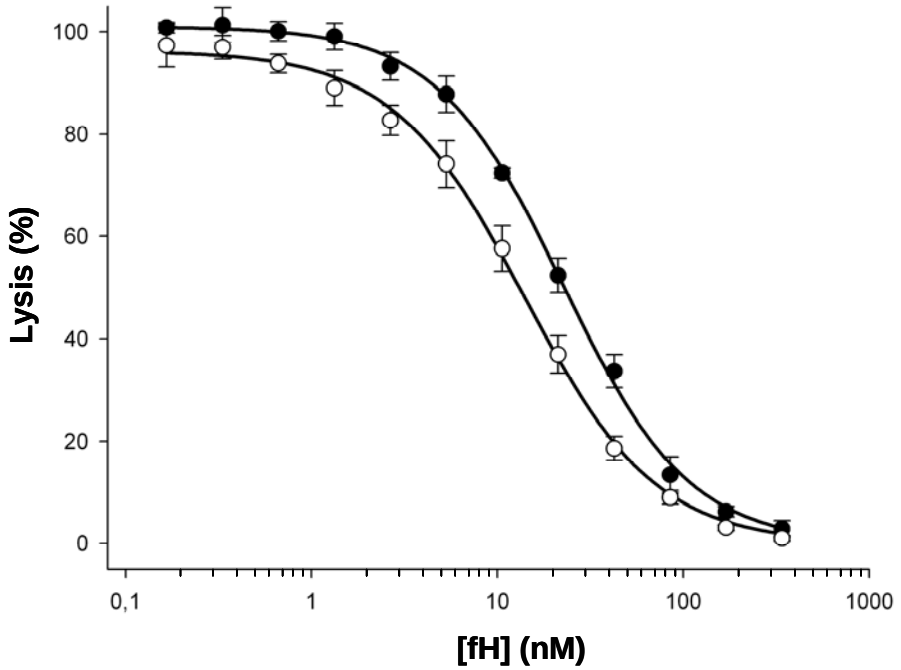

Figure 4

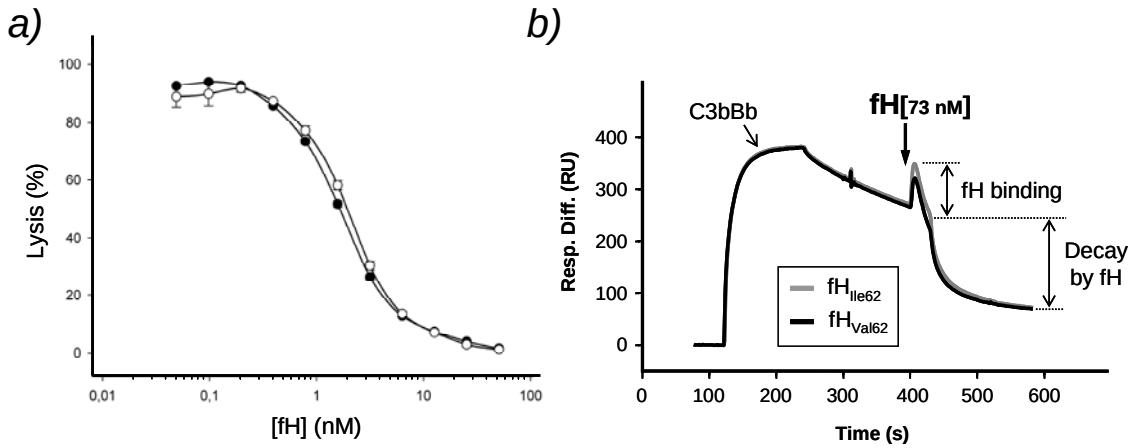
a)
b)
Lysis (%)
[fH] (nM)
C3bBb
fH[73 nM]
fH binding
Decay by fH
Resp. Diff. (RU)
Time (s)
fH Ile62
fH Val62

Figure 5

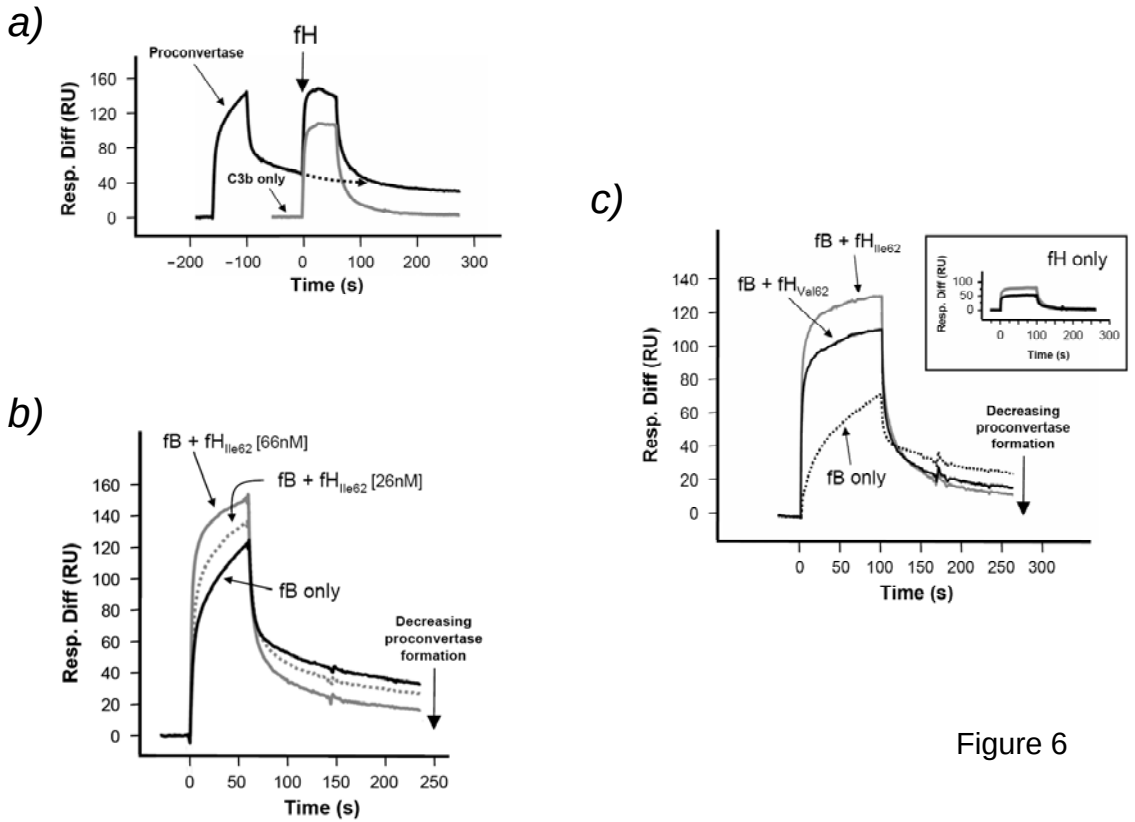
a)
Proconvertase
fH
C3b only
Resp. Diff (RU)
Time (s)
b)
fB + fH Ile62 [66nM]
fB + fH Ile62 [26nM]
fB only
Decreasing proconvertase formation
Resp. Diff (RU)
Time (s)
c)
fB + fH Ile62
fB + fH Val62
fH only
fB only
Decreasing proconvertase formation
Resp. Diff (RU)
Time (s)

Figure 6

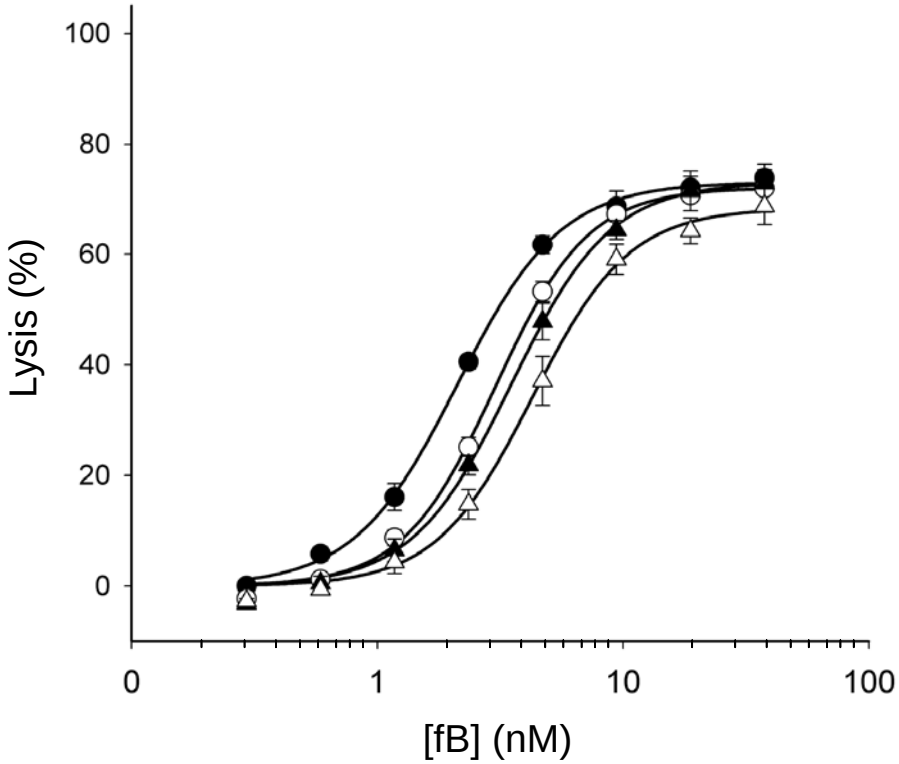

Figure 7